Additive Manufacturing Letters 13 (2025) 100272

Contents lists available at ScienceDirect

Additive Manufacturing Letters

journal homepage: www.elsevier.com/locate/addlet

Short Communication

Investigation on curing strategies for metal binder jetting with Ti-6Al-4V

Kevin Janzen [a,*], Timo Rieß [a], Claus Emmelmann [b]

[a] Fraunhofer Research Institution for Additive Manufacturing Technologies IAPT, Am Schleusengraben 14, 21029 Hamburg, Germany
[b] Institute of Laser and System Technologies (iLAS), Hamburg University of Technology TUHH, Harburger Schloßstr. 28, 21079 Hamburg, Germany

ARTICLE INFO

Keywords:
Metal binder jetting
Curing
Titanium alloys, medical technology, process qualification

ABSTRACT

Metal binder jetting is a promising manufacturing technology that holds the potential to be a future competition technology to classic laser based additive manufacturing processes. In contrast to these technologies, however, metal binder jetting is much less mature. While sintering and debinding are already well known due to the spread of metal injection molding and powder deposition by laser powder bed fusion and its related processes, the often-neglected curing step represents a major challenge in process control. This study was therefore the first comprehensive investigation into the curing of metal binder jetting green parts from Ti-6Al-4 V powder with a powder size distribution below 25 µm. It was shown that the curing step has only a minor effect on the green part quality (surface roughness and density), but at the same time has a decisive influence on the green strength. In addition, position-dependent effects for the green density were detected, which indicate insufficient curing in the outer areas of the print box.

1. Introduction

Metal binder jetting is an additive manufacturing (AM) technique that builds complex parts layer-by-layer by selectively depositing a liquid binder onto a bed of metal powder [1,2]. Unlike fusion-based methods such as selective laser powder bed fusion (L-PBF) or electron powder bed fusion (E-PBF), binder jetting does not require high temperatures to melt the metal, allowing parts to be manufactured without the thermal stresses typically associated with these high-energy processes. This makes binder jetting particularly well-suited for materials that are sensitive to high temperatures such as titanium alloys like Ti-6Al-4 V, which are widely used in aerospace, medical, and industrial applications for their high strength-to-weight ratio and corrosion resistance [3].

The process of metal binder jetting begins with spreading a thin layer of powder across the build platform, after which a printhead selectively deposits droplets of binder according to a 3D model. This binder temporarily holds the powder particles together, forming a "green part" [1,2]. However, the green part at this stage is fragile and requires stabilization before undergoing the high-temperature sintering process that densifies the material. Curing, the process of heating the green part at low temperatures, plays a crucial role in binder jetting. During curing, the binder hardens, providing structural integrity to the green part so it can withstand handling and subsequent post-processing [1]. Curing parameters such as temperature, time, and atmosphere affect the binder's polymerization, the dimensional stability of the part, and ultimately the quality of the final sintered component. Effective binder migration through controlled heating ensures that the binder's volume and composition are managed, reducing the risk of distortion, swelling, or porosity in the final sintered part. It also has a major influence on the subsequent de-powdering of the green parts, as incomplete migration can lead to powder sticking or clumping.

The curing process must carefully control thermal transitions to avoid damaging the green part or causing premature degradation of the binder. Commonly, curing temperatures range between 150 °C and 250 °C, well below the melting points of most metal powders, to minimize any risk of sintering or (especially in the case of titanium alloys) pick up of oxygen or other impurities [4]. Within this temperature range, binders typically undergo different transformations. Many binders used in MBJ rely on polymerizable compounds that form stable networks through cross-linking reactions when exposed to heat [5]. Polymerization strengthens the binder, enhancing the green part's stability and resistance to mechanical stresses [2,6–8]. Some binders experience a glass transition temperature (T_g), where the material softens without fully melting. At T_g, the binder transitions from a brittle, glassy state to a softer, more ductile state, allowing the binder to conform to the particle surfaces and improve contact among metal particles [9]. As the binder is cooled below T_g or partially cross-linked, it solidifies, forming a rigid

* Corresponding author.
E-mail address: kevin.janzen@iapt.fraunhofer.de (K. Janzen).

https://doi.org/10.1016/j.addlet.2025.100272
Received 26 November 2024; Received in revised form 30 December 2024; Accepted 23 January 2025
Available online 25 January 2025

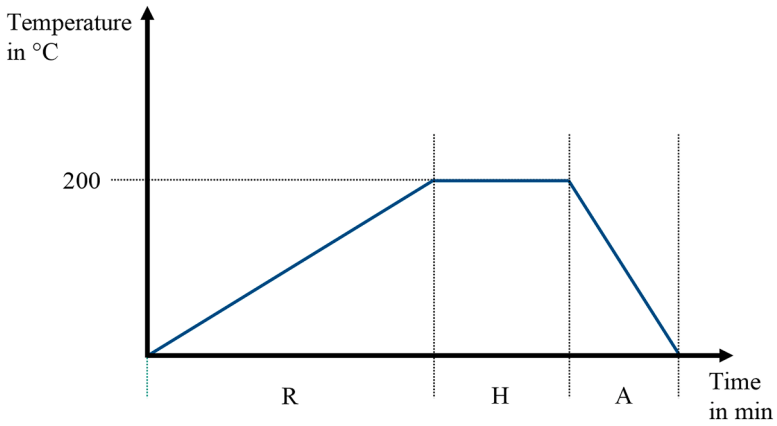

Fig. 1. Exemplary curing cycle [4].

structure that holds the green part's shape [6,7,10]. The binder's solidified state is crucial to withstand subsequent handling, transport, and sintering. During curing, binders containing water or solvent molecules may also experience dehydration, releasing any residual moisture from the green part. Dehydration and solvent removal ensure that the green part maintains dimensional accuracy, minimizing risks of shrinkage or cracking during sintering [8,11,12]. Thermal transitions must be carefully managed to retain the green part's integrity and minimize stress [13]. Rapid heating can cause binder cracking or delamination, while overly prolonged curing times may reduce dimensional precision due to binder softening.

The curing atmosphere – whether air, inert gas, or vacuum – plays an important role in the stability and quality of the green part during curing. So far, this influence has been little researched and curing usually takes place under air [8,11,14,15]. Different atmospheres influence the binder's behavior, the rate of oxidation, and potential reactions with other environmental components [11]:

Ambient atmosphere: Curing in air allows for some level of oxidation, which may stabilize the green part but can also introduce surface oxidation on some metal powders. This can be beneficial to degrade the binder more efficiently, though it can also introduce contaminants that might impact final mechanical properties [16].

Inert gas atmosphere: Curing in an inert gas environment, such as nitrogen or argon, reduces the risk of oxidation, preserving the purity of the metal particles and binder composition. This is often preferred for reactive metals like titanium alloys (e.g., Ti-6Al-4 V) where oxidation could compromise part performance.

Vacuum curing: Vacuum environments offer effective solvent removal and binder stabilization without atmospheric interference, making them suitable for sensitive materials. Vacuum curing can also reduce residual stresses by enabling uniform binder hardening throughout the green part.

Selecting an appropriate atmosphere depends on the binder type and the specific alloy being printed. Curing parameters such as temperature, duration, and heating rate are central to achieving optimal binder migration and green part stabilization. The temperature and time are interdependent; higher curing temperatures can reduce the required curing time but may increase the risk of binder degradation or dimensional warping [10]. Conversely, lower temperatures require extended curing durations but often yield more stable green parts. The curing temperature is generally set just above the binder's glass transition temperature to ensure solidification without excessive decomposition [17]. For Ti-6Al-4 V, typical curing temperatures are chosen to optimize the green part's structural stability, balancing binder hardening against the risk of oxidation [4].

Optimized curing prevents binder migration and cracking, leading to smoother surfaces in the green part. A high-quality surface finish in the green state can reduce the need for extensive post-processing, improving production efficiency [18,19]. Determining a suitable temperature profile for curing is also often a trade-off between higher green part strength and better powder removal. A single temperature profile can produce a high green part strength but at the same time lead to an excessive amount of adhering powder due to unfavourable binder mitigation, which makes subsequent depowdering more difficult [20].

Table 1
Properties of the investigated powder.

Alloy	Supplier	D_{10} (µm)	D_{50} (µm)	D_{90} (µm)	Apparent Density (g/cm^3)	Tap Density (g/cm^3)
Ti-6Al-4V	Tekna	9.43 [1]	15.6 [1]	21.3 [1]	≥2.1 [2]	≥2.7 [2]

[1] Measured using dynamic image analysis;.
[2] Manufacturer information; apparent density according to ASTM B527 and Tap density according to ASTM B417.

In summary, the principles behind curing in metal binder jetting involve balancing binder transformation, thermal transitions, and environmental control to stabilize the green part before sintering. The optimization of curing parameters directly impacts final part properties, making curing a critical focus area for advancing metal binder jetting applications, particularly for sensitive materials like Ti-6Al-4 V. By understanding and controlling these principles, binder jetting can achieve consistent, high-quality parts suitable for industrial and medical applications.

A typical curing cycle is shown in Fig. 1. It is divided into a ramp time (R), a holding time (H) and the cooling time (A).

In this study, we explore different curing strategies specifically for Ti-6Al-4 V, assessing how variations in curing parameters influence the mechanical properties and dimensional accuracy of binder-jetted parts. The results are intended to optimize curing protocols, ensuring that parts retain dimensional stability and meet industrial performance standards after sintering. The present work is part of a series of studies that serve to provide a holistic view of the MBJ process with Ti-6Al-4 V and are intended to advance the industrial maturity of the process for use in medical technology [4,21–23].

2. Materials & methods

In this chapter the realization of the experiments is described. In addition to the experiments themselves, measurement methods and test specimens are also explained.

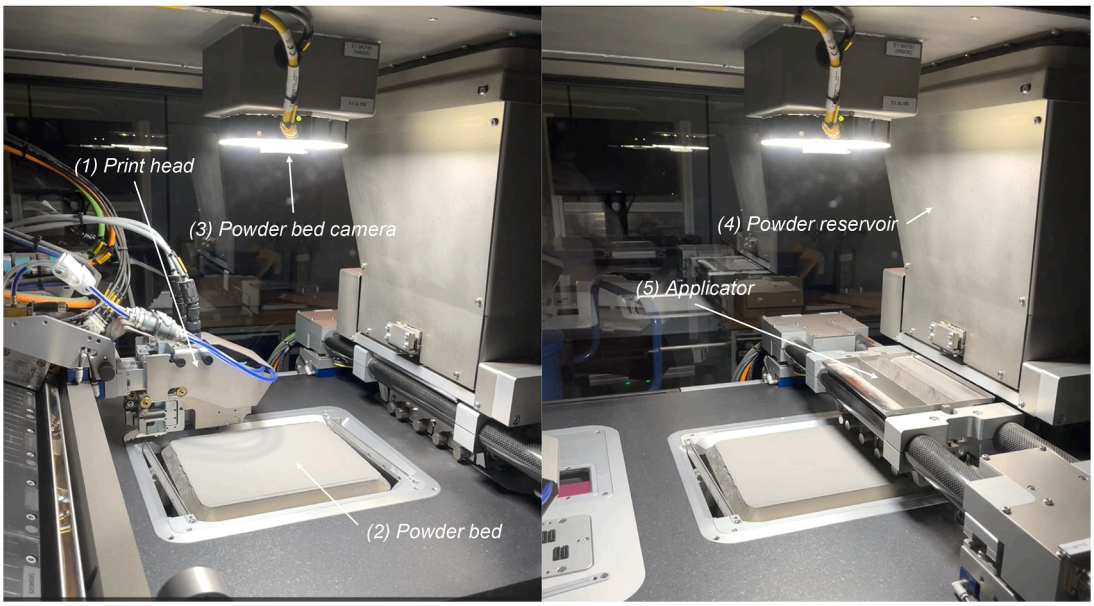

Fig. 2. Configuration of MBJ system Markforged DMP2500.

Table 2
Process parameters for MBJ.

Parameter	Value
Layer thickness	42 µm
Print box temperature	80 °C
Powder magazine temperature	70 °C
Print speed	200 mm/s
Powder application speed	30 mm/s

2.1. Materials

In order to investigate the curing with a high relevance to medical technology, a plasma-atomized spherical Ti-6Al-4 V powder from Tekna Advanced Materials, Inc., was selected, which is used industrially for metal powder injection molding of medical components. The most important characteristic properties of the powder are shown in Table 1.

The analyzed binder is C20 from Markforged. The exact composition of the binder is confidential, but according to the safety data sheet it is a water-based system with triethylene glycol as the main component in addition to alcohol and an unknown surfactant.

2.2. Binder jetting

To produce specimen for the latter investigations on curing a MBJ system (DMP2500) from Markforged was used. The system is shown in Fig. 2. Here, the binder is applied to the powder bed (2) using a thermal 2-head print head system (1). The process is monitored with the help of a permanently installed camera system (3). Once the binder has been applied, the powder bed is lowered and a vibration-controlled applicator applies the next layer of powder by using a blade recoater. The applicator (5) is filled via a top feeder reservoir (4). These steps are repeated for every layer to subsequently build up the desired part geometry.

As the investigation was to focus solely on the curing step, the printing parameters for the MBJ process were left unchanged for all experiments. The process parameters used are summarized in Table 2:

Powder conditioning before printing was done as described in our previous work [23].

2.3. Test specimen and measuring methods

In order to derive suitable test specimens, the to-be-measured variables must first be defined. As already described in the introduction, the process development for curing strategies often involves a trade-off between green part strength and depowdering properties. Therefore, these two factors should be at the centre of the investigation. In addition, the density of green parts and the surface roughness were analysed as central elements for assessing the general quality of green parts.

Green part density was measured geometrically using fringe projection, a triangulation-based optical method. In this technique, structured light in the form of fringes illuminates the part, and a camera captures the diffraction pattern. The known positions of the camera and the projector enable the precise triangulation of the component's surface, allowing the volume to be calculated accurately. The fringe projection system used (VR-6200 by Keyence Corporation) achieves a measurement accuracy of 4 µm at twenty-fold magnification using a macro camera. Factors affecting the accuracy include room lighting and the reference surface used for measurement. To ensure consistency, the lighting was kept constant, and the object table served as the reference surface. The sample's weight was determined using a precision balance

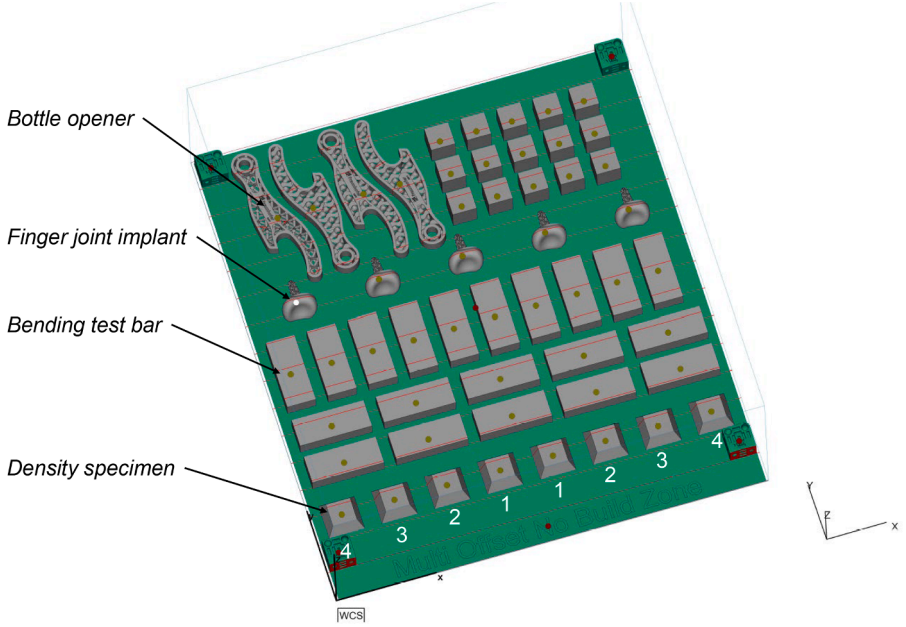

Fig. 3. Print job setup including test specimen.

(PRACTUM 124–1S by Sartorius), enabling the calculation of the geometric green density. This approach provides a non-destructive and precise method for evaluating green part density [4]. Derived from the measurement method, a pyramid with a flat top is used as the test body. The base of the pyramid has an edge length of 14 mm.

Surface roughness was also assessed using the fringe projection system. The structured light technique allows detailed mapping of the component's geometry, ensuring that any deviations or irregularities in the green part's dimensions and surface quality can be quantified with high precision. The green part strength was evaluated through a bending test conducted in accordance with DIN EN ISO 3995. Although this standard is intended for metallic pressed parts, it is commonly adapted for green parts in the absence of specific standards. The test setup involved placing the green part on two support cylinders spaced 25 mm apart and applying a central load to induce bending. A tensile/compression testing machine (ZwickRoell 10 kN) was used, equipped with an appropriate bending test fixture. The sample geometry is a bar with the dimensions 30×12×9 mm. This method provides reliable insights into the mechanical properties of green parts, which are critical for assessing their handling and performance during post-processing.

As there is no specific measurement method for evaluating depowderability, two exemplary components with geometries typical of the MBJ process were included in the test series. The first component is a prototype of a finger joint implant with an osseointegrative TPMS structure and a smooth joint surface [22]. The second test component is a bottle opener with a bionic internal structure with many undercuts and thin crossbars. In order to analyse the curing process depending on the position, the test specimens for density determination are assigned numbers from 1 to 4, with 1 corresponding to a position on the very inside of the print bed and 4 on the very outside. All test specimen and the used print job setup are shown in Fig. 3. Bending and density samples are distributed along the X-axis in order to include positional influences during curing in the investigation. However, in order to keep the tests economical, the Y-axis is not included. In the corners of the print box, reserve specimens with a defined geometry are always printed. These samples are not part of the test.

2.4. Curing

The curing step, which is often the most neglected process step and has hardly been investigated to date, is usually based on the pragmatic recommendations of the binder manufacturer. In the case of the Markforged C20 binder used for this study, the following process is therefore considered standard procedure when using a convection furnace:

$$R(L) = I + L \cdot 0,3 \tag{1}$$

$$H(L) = \begin{cases} 1h, & L < 300 \\ 2h, & 300 \leq L < 600 \\ 3h, & L \geq 600 \end{cases} \tag{2}$$

The variable R here refers to the ramp of the temperature function in minutes and depends on the number of layers L and the total binder quantity in grams I. The holding time H is only estimated on the basis of the number of layers L. The parameters used and their units already show that the basis of the calculation is an empirical rule of thumb and does not reflect any physical relationships. For this study, a vacuum drying furnace (Memmert VO49) based on the heat conduction principle was used as an alternative to the standard convection furnace. This makes it possible to carry out curing tests not only under air but also under nitrogen or vacuum.

It is assumed that a beneficial relationship between layer thickness and holding time is approximately linear. Therefore, the specification of the holding time H is converted into linear equations for finer adjustment and observations during the experiments. Two linear functions can

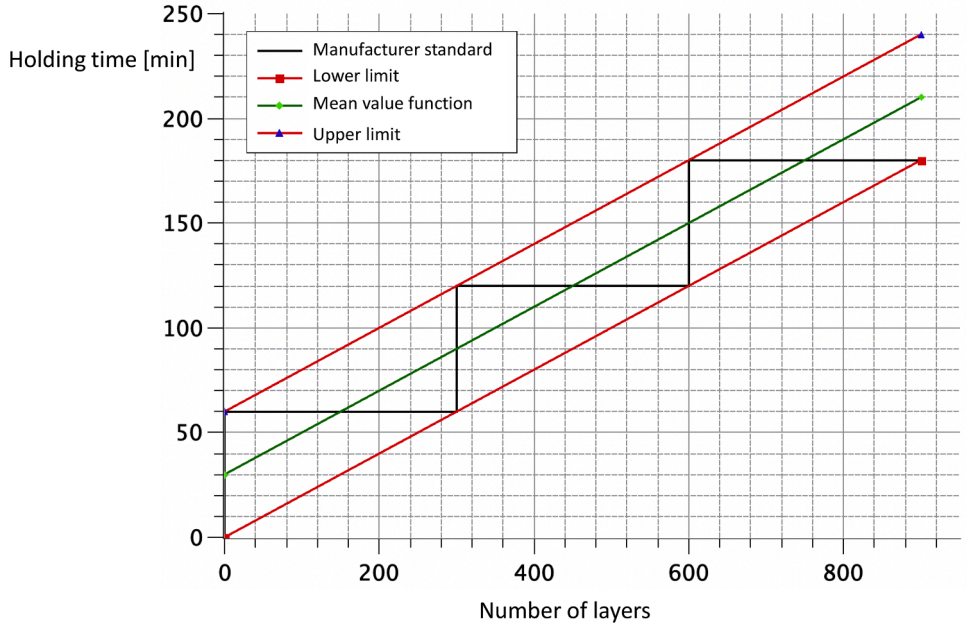

Fig. 4. Curing functions.

be formed from the specified holding times, which span the recommended time period with the upper limit function $O(L)$ and the lower limit function $U(L)$. In addition, a mean value function $M(L)$ is obtained (see Fig. 4):

This results in the following equations for determining the holding time H:

$$\mathrm{O(L)} = 0,2\,\mathrm{L} + 60 \tag{3}$$

$$\mathrm{U(L)} = 0,2\,\mathrm{L} \tag{4}$$

$$\mathrm{M(L)} = 0,2\mathrm{L} + 30 \tag{5}$$

For the experiments, 3 different holding times were tested with a constant layer thickness, using the upper limit range, the lower limit range and the mean value. In this way, the entire range of the recommended space is tested. In addition to the holding time H, the ramp R time is also adjusted. To do this, the last factor in the original formula is varied. The two stages look as follows:

$$R = I + L \cdot 0,2 \tag{6}$$

$$R = I + L \cdot 0,3 \tag{7}$$

The three-stage design allows non-linear trends to be recognised. This results in the following test plan (shown in Table 3), based on the Box Behnken design, in which extreme value combinations are omitted to avoid uncertainties [24,25]. The aim of the test plan is to map different ramps and holding times as a function of the binder quantity and the number of layers in order to ultimately develop a practical curing strategy for the investigated Ti-6Al-4 V powder. The test plan is also divided in experiments under air and under nitrogen atmosphere to investigate their influence as well.

Table 3
Test plan.

Test no.	Sequence	Ramp time R [min]	Holding time [min]	Atmosphere
A1	2	$R = I + L$ x 0,2	$\mathrm{M(L)} = 0,2\,L + 30$	Air
A2	7	$R = I + L$ x 0,3	$\mathrm{U(L)} = 0,2\mathrm{L}$	Air
A3	5	$R = I + L$ x 0,3	$\mathrm{O(L)} = 0,2\,L + 60$	Air
A4	1	$R = I + L$ x 0,3	$\mathrm{M(L)} = 0,2\,L + 30$	Air
N1	6	$R = I + L$ x 0,2	$\mathrm{M(L)} = 0,2\,L + 30$	Nitrogen
N2	3	$R = I + L$ x 0,3	$\mathrm{U(L)} = 0,2\mathrm{L}$	Nitrogen
N3	8	$R = I + L$ x 0,3	$\mathrm{O(L)} = 0,2\,L + 60$	Nitrogen
N4	4	$R = I + L$ x 0,3	$\mathrm{M(L)} = 0,2\,L + 30$	Nitrogen

Table 4
Test plan including calculated ramp and holding times.

Test no.	Sequence	Ramp time R [min]	Holding time [min]	Atmosphere
A1	2	114	88	Air
A2	7	143	58	Air
A3	5	143	118	Air
A4	1	143	88	Air
N1	6	114	88	Nitrogen
N2	3	143	58	Nitrogen
N3	8	143	118	Nitrogen
N4	4	143	88	Nitrogen

The number of layers for the respective test print job (see Fig. 3) is $L = 289$ and the quantity of binder is $I = 56\ g$. Both values stay the same for every run because test print setup and print parameters (see 2.2) were kept constant. This results in the final test conditions, which are summarised in Table 4:

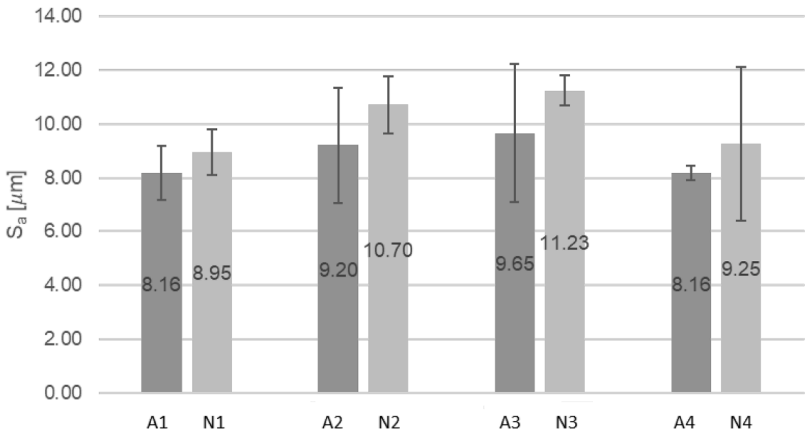

Fig. 5. Surface roughness S_a with standard deviations.

3. Results & discussion

In this section, the results of every experiment are summarized and discussed.

3.1. Green part quality

The surface roughness S_a and the green density ρ_G are used to compare the green part quality for the different curing cycles. Initially, there is no significant difference between the experiments for surface roughness (see Fig. 5).

The same applies to the green density (see Fig. 6).

More interesting, however, is a look at the positional influence of the samples (shown in the figure). Here it is clear that the outermost samples in particular have a significantly higher density of green parts. Although an increase in the green part density is usually desirable, in this case it is more an indication of inefficient curing, as it can be assumed that the packing density of the powder is equally distributed throughout the powder bed. One possible explanation for this would be a restriction of binder evaporation through the side walls of the print box (see Fig. 7).

3.2. Green strength

Perhaps the most important evaluation factor for the success of a curing process is the green strength. A high green strength leads directly to fewer rejects because fewer green bodies are damaged during depowdering and there is a higher potential for automation for future industrial applications with larger quantities. Large differences between the individual curing strategies are recognisable for the green strength. Fig. 8 shows the results of the 3-point bending tests.

The measurement results show that both the atmosphere and in particular, the temperature curve have a major influence on the strength

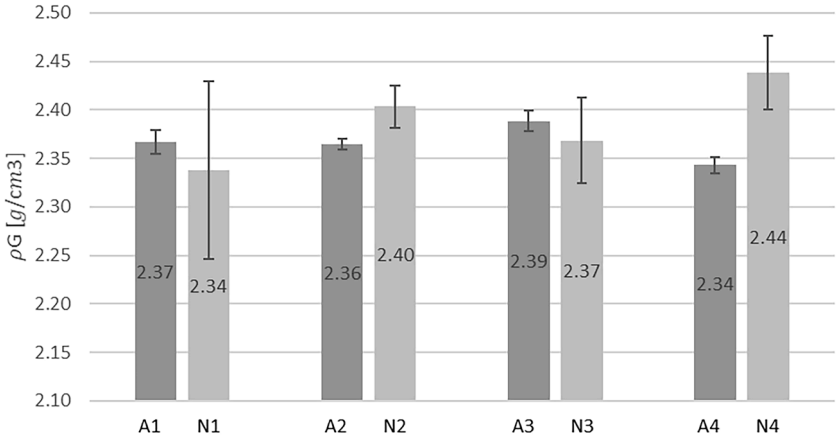

Fig. 6. Green density ρ_G with standard deviations.

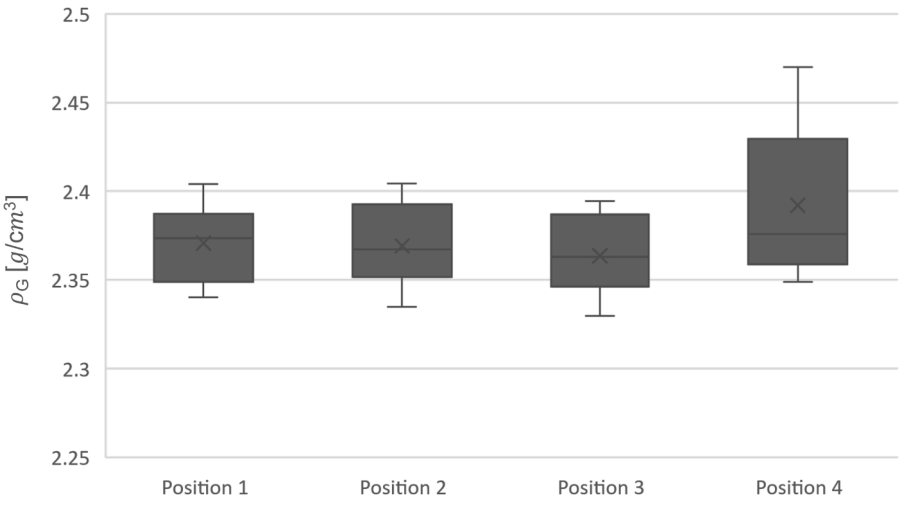

Fig. 7. Green density ρ_G for different positions.

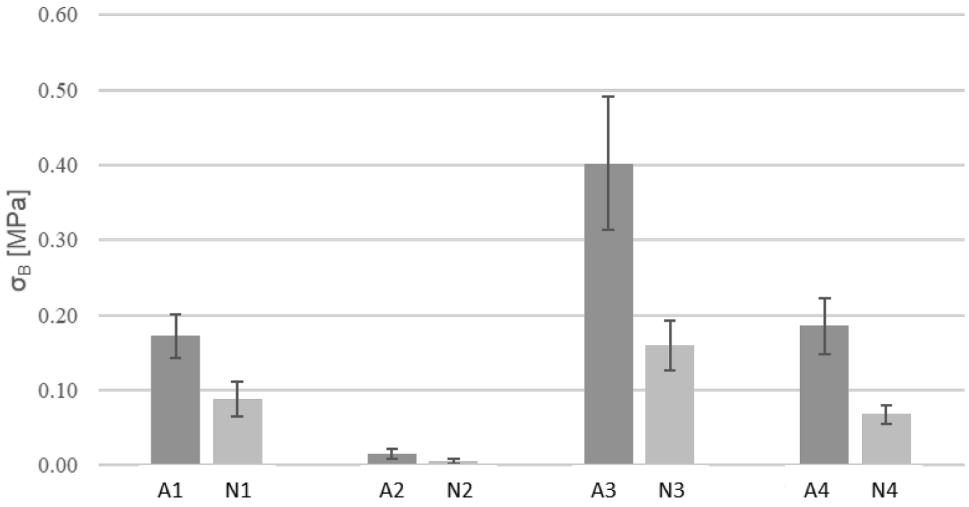

Fig. 8. Green strength σ_B for different curing strategies and atmospheres.

Table 5
Depowder rating for every experiment.

Test no.	A1	A2	A3	A4	N1	N2	N3	N4
Holding time [min]	88	58	118	88	88	58	118	88
Ramp time [min]	114	143	143	143	114	143	143	143
Rating	2	2	5	3	2	2	5	3

of the green parts. The transitions described under 1 are strongly influenced by temperature profiles. In addition, the general stabilisation under ambient atmosphere already described can be seen in the measurement results, as the samples that were cured under nitrogen generally have lower strength values. In contrast to oxygen, the inert nitrogen atmosphere inhibits reactions that can lead to the degradation of substances in the binder and solvent. This could slow down the hardening of the polymer.

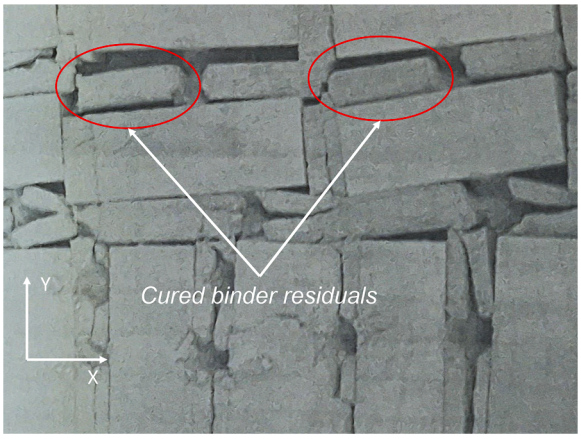

Fig. 9. Exemplary photo from the depowdering process showing cured residual binder.

3.3. Depowdering

The effects of the different process variants cannot only be assessed on the basis of measurable variables. The behaviour of the green parts and the surrounding powder during depowdering is of crucial importance for the future successful implementation. Each depowdering process was documented and any anomalies were noted. In each case, a rating of 1–5 was derived from this, whereby 1 corresponds to a particularly large amount of adhesive powder, while 5 corresponds to

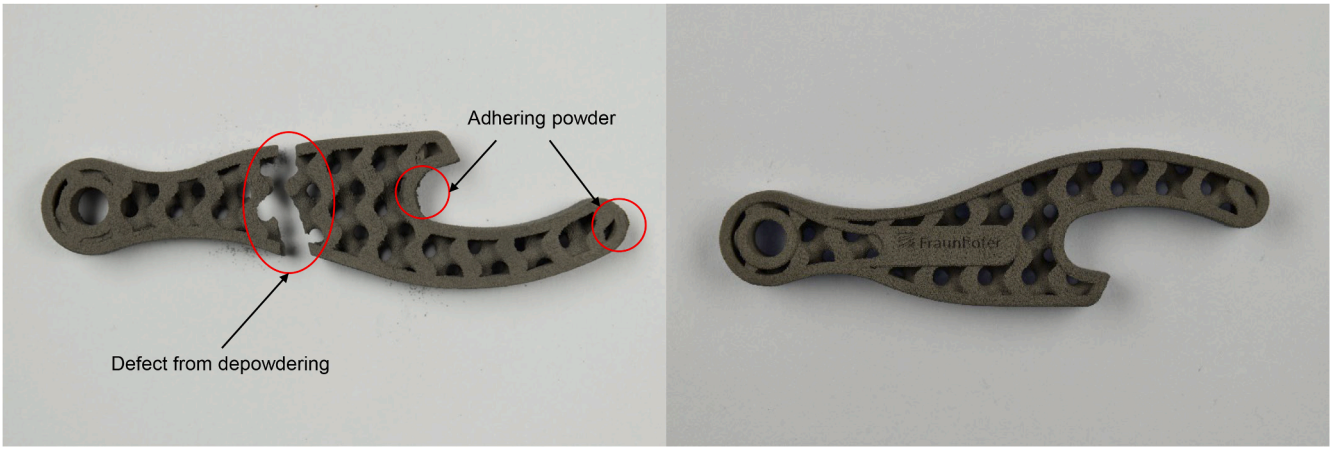

Fig. 10. Exemplary green samples from depowdering experiments A2 (left) and A3 (right).

subjective flow properties similar to new powder (see Table 5). The following findings are neither measurable nor fully verifiable; they are largely based solely on the authoress's perception. The evaluation shows that, in principle, longer holding times in particular lead to better depowdering. This is due on the one hand to the greater stability of the green parts (see also 3.2) and on the other hand to more effective evaporation of the binder, as a result of which the surrounding powder adheres less or clumps together.

Fig. 9 shows how lumps of powder form, particularly in narrow spaces between components, which indicate binder residues (combined with particle interlocking). These lumps can be explained by two effects: Firstly, depending on the curing temperature, the binder migration already described in the introduction occurs to a greater or lesser extent and leads to binder becoming trapped in the powder surrounding the components. On the other hand, a kind of smearing can occur during printing. This is caused by the particles floating when the binder is applied. If the recoater then applies the next layer of powder, some of the wetted powder smears and forms areas that later clump together during curing. Powder clumping of the magnitude shown cannot be explained purely by particle interlocking, because this only occurs in the vicinity of printed components and, due to the blade coater, no increased forces are exerted on the powder bed (in contrast to a roller recoater).

Fig. 10 shows on the left an exemplary bottle opener from test A2 with a particularly short holding time, clearly adhering powder and a defect caused by the low green strength during de-powdering. The same component from test A3 is shown on the right side for comparison. This illustrates typical damage that occurs during de-powdering as a result of insufficient green strength as shown in Fig. 8.

4. Conclusion

This study highlights the significant role that curing strategies play in enhancing the quality of green parts produced via MBJ using Ti-6Al-4 V. The results indicate that while curing parameters such as temperature profiles and atmosphere considerably influence green strength—critical for handling and further processing—their impact on surface roughness and green density is relatively minor. This suggests that the initial powder distribution and compaction are primary determinants of these properties.

Importantly, the research highlights position-dependent effects within the build area, where parts located at the edges exhibit higher green densities compared to those in central positions. This observation raises concerns about potential non-uniform curing conditions, likely caused by uneven heat distribution due to the print box walls, which may lead to inconsistent mechanical properties across the build.

To advance future studies, it is essential to conduct detailed comparisons among various curing strategies aimed at optimizing specific properties. Researchers should focus on identifying the optimal curing temperature, duration, and atmosphere that best enhance green strength specific to their used binder system and application while ensuring uniformity across different positions within the build area. The results of the study suggest that long holding times of more than 2 h make sense for MBJ components of typical size, while ramp times can be chosen short to create a more time-efficient process.

Future investigations should also consider a broader range of binder-material combinations to establish comprehensive guidelines for the industrialization of MBJ technology, particularly in the medical sector. The present results are based on the water-based binder C20 from Markforged. The results shown can therefore be transferred particularly well to other water-based binder systems. How the mechanisms discussed work for phenolic or solvent-based binders, for example, should be investigated in future studies. By refining curing chamber designs and process parameters, researchers can address positional inconsistencies and improve the reliability of MBJ for industrial applications. Ultimately, this study serves as a foundational step towards establishing a more mature and effective MBJ process for Ti-6Al-4 V, paving the way for enhanced applications in the medical technology field and beyond.

CRediT authorship contribution statement

Kevin Janzen: Writing – original draft, Visualization, Validation, Methodology, Investigation, Formal analysis, Data curation, Conceptualization. **Timo Rieß:** Visualization, Validation, Methodology, Investigation, Formal analysis, Data curation. **Claus Emmelmann:** Writing – review & editing, Supervision.

Declaration of competing interest

The authors declare that they have no known competing financial interests or personal relationships that could have appeared to influence the work reported in this paper.

Acknowledgements

This work was supported by the Fraunhofer Internal Programs under Grant No. PREPARE 840226.

Data availability

Data will be made available on request.

References

[1] I. Gibson, D. Rosen, B. Stucker, M. Khorasani, Additive Manufacturing Technologies, Springer International Publishing, Cham, 2021.

[2] E. Sachs, M. Cima, P. Williams, D. Brancazio, J. Cornie, Three dimensional printing: rrapid tooling and prototypes directly from a CAD model, Journal of Engineering for Industry 114 (1992) 481–488, https://doi.org/10.1115/1.2900701.

[3] A. Simchi, F. Petzoldt, T. Hartwig, S.B. Hein, B. Barthel, L. Reineke, Microstructural development during additive manufacturing of biomedical grade Ti-6Al-4V alloy by three-dimensional binder jetting: material aspects and mechanical properties, Int. J. Adv. Manuf. Technol. 127 (2023) 1541–1558, https://doi.org/10.1007/s00170-023-11661-1.

[4] K. Janzen, K.J. Kallies, L. Waalkes, P. Imgrund, C. Emmelmann, Recycling of Ti-6Al-4V powder in metal binder jetting, in: WorldPM2024 Yokohama Proceedings, 2024.

[5] T. Saito, A.M. Elliott, D.T. Brunermer, D.B. Gilmer, M. Lehmann, H. Yu US11254617B2, 2020.

[6] M. Ziaee, N.B. Crane, Binder jetting: a review of process, materials, and methods, Addit. Manuf. 28 (2019) 781–801, https://doi.org/10.1016/j.addma.2019.05.031.

[7] R. Patterson, D.H. Hollenberg, R.C. Desjarlais, G.E. Alderfer US4732786A, 1988.

[8] A. Mostafaei, A.M. Elliott, J.E. Barnes, F. Li, W. Tan, C.L. Cramer, P. Nandwana, M. Chmielus, Binder jet 3D printing—Process parameters, materials, properties, modeling, and challenges, Prog. Mater. Sci. 119 (2021) 100707, https://doi.org/10.1016/j.pmatsci.2020.100707.

[9] T.L. Yu, Glass transition temperature profile of the curing reaction, Polym. J. (1996) 965–969.

[10] M.P. Watters, M.L. Bernhardt, Modified curing protocol for improved strength of binder-jetted 3D parts, Rapid. Prototyp. J. 23 (2017) 1195–1201, https://doi.org/10.1108/RPJ-09-2016-0146.

[11] K. Zissel, Influence of the processing atmosphere on binder jetting of stainless steel: ffrom printing to sintering. THESIS FOR THE DEGREE OF LICENTIATE OF ENGINEERING, Gothenburg, Sweden, 2024.

[12] T.J. Ayres, S.R. Sama, S.B. Joshi, G.P. Manogharan, Influence of resin infiltrants on mechanical and thermal performance in plaster binder jetting additive manufacturing, Addit. Manuf. 30 (2019) 100885, https://doi.org/10.1016/j.addma.2019.100885.

[13] T. Do, P. Kwon, C.S. Shin, Process development toward full-density stainless steel parts with binder jetting printing, Int. J. Machine Tools. Manuf. 121 (2017) 50–60, https://doi.org/10.1016/j.ijmachtools.2017.04.006.

[14] H. Miyanaji, S. Zhang, A. Lassell, A. Zandinejad, L. Yang, Process development of porcelain ceramic material with binder jetting Process for dental applications, JOM 68 (2016) 831–841, https://doi.org/10.1007/s11837-015-1771-3.

[15] S. Mirzababaei, S. Pasebani, A review on binder jet additive manufacturing of 316L stainless steel, JMMP 3 (2019) 82, https://doi.org/10.3390/jmmp3030082.

[16] J. Izdebska, Aging and degradation of printed materials. Printing On Polymers, Elsevier, 2016, pp. 353–370.

[17] R. Carbas, L.Da Silva, E. Marques, A.M. Lopes, Effect of post-cure on the glass transition temperature and mechanical properties of epoxy adhesives, J. Adhes. Sci. Technol. 27 (2013) 2542–2557, https://doi.org/10.1080/01694243.2013.790294.

[18] A. Lores, N. Azurmendi, I. Agote, E. Espinosa, M.B. García-Blanco, A study of parameter and post-processing effects on surface quality improvement of Binder Jet 3D-printed Invar36 alloy parts, Prog Addit Manuf 7 (2022) 917–930, https://doi.org/10.1007/s40964-022-00267-w.

[19] A. Lores, N. Azurmendi, I. Agote, E. Zuza, A review on recent developments in binder jetting metal additive manufacturing: materials and process characteristics, Powder Metallurgy 62 (2019) 267–296, https://doi.org/10.1080/00325899.2019.1669299.

[20] Z. Zhou, A. Lennon, F. Buchanan, H.O. McCarthy, N. Dunne, Binder jetting additive manufacturing of hydroxyapatite powders: eeffects of adhesives on geometrical accuracy and green compressive strength, Addit. Manuf. 36 (2020) 101645, https://doi.org/10.1016/j.addma.2020.101645.

[21] K. Janzen, P. Groß, P. Imgrund, C. Emmelmann, Potentials of metal binder jetting process chains for medical parts, in: World PM2022 Lyon Proceedings, 2022.

[22] K. Janzen, K.J. Kallies, Fabrication of patient-specific finger joint implants from Ti-6Al-4V using metal binder jetting. 830 pages */transactions on Additive Manufacturing meets Medicine*, vol. 5 No. 1 (2023), Trans. AMMM, Trans. Additive Manuf. Meets Medicine (2023), https://doi.org/10.18416/AMMM.2023.2309830.

[23] K. Janzen, K.J. Kallies, L. Waalkes, P. Imgrund, C. Emmelmann, Influence of different powder conditioning strategies on metal binder jetting with Ti-6Al-4V, Materials. (Basel) 17 (2024), https://doi.org/10.3390/ma17030750.

[24] K. Siebertz, D. van Bebber, T. Hochkirchen, Statistische Versuchsplanung, Springer Berlin Heidelberg, Berlin, Heidelberg, 2010.

[25] S.L.C. Ferreira, R.E. Bruns, H.S. Ferreira, G.D. Matos, J.M. David, G.C. Brandão, E. G.P. Da Silva, L.A. Portugal, P.S. dos Reis, A.S. Souza, W.N.L. dos Santos, Box-Behnken design: an alternative for the optimization of analytical methods, Anal. Chim. Acta 597 (2007) 179–186, https://doi.org/10.1016/j.aca.2007.07.011.